



Cite this: *RSC Adv.*, 2018, 8, 28555

# Effects of calcination and pretreatment temperatures on the catalytic activity and stability of H<sub>2</sub>-treated WO<sub>3</sub>/SiO<sub>2</sub> catalysts in metathesis of ethylene and 2-butene

Krittidech Gayapan, Sirada Sripinun, Joongjai Panpranot,  Piyasan Praserttham and Suttichai Assabumrungrat \*

The effects of calcination and pretreatment temperatures of the H<sub>2</sub>-treated WO<sub>3</sub>/SiO<sub>2</sub> catalysts in metathesis of ethylene and 2-butene to propylene were investigated. The results showed that pretreatment with pure hydrogen over the non-calcined catalysts resulted in higher activity and stability than the calcined catalysts, and the hydrogen pretreatment temperature at 650 °C offered the highest 2-butene conversion and propylene selectivity. The calcination of the catalyst before hydrogen pretreatment was proved to be unnecessary. As revealed by various characterization results from N<sub>2</sub> physisorption, XRD, TEM, UV-Vis, Raman, *in situ* H<sub>2</sub>-TPR, *in situ* NH<sub>3</sub>-DRIFTS and *in situ* NH<sub>3</sub>-TPD techniques, activity of the metathesis of ethylene and 2-butene to propylene was related to tungsten dispersion on the support, WO<sub>2.83</sub> and WO<sub>2</sub> phase composition, and isolated surface tetrahedral tungsten oxide species. The stability of the metathesis reaction was also related to the total acidity and the acid sites of both Brønsted and Lewis acid sites.

Received 10th June 2018  
Accepted 5th August 2018

DOI: 10.1039/c8ra04949a

rsc.li/rsc-advances

## 1. Introduction

Propylene is an important chemical intermediate serving as a building block for petrochemical and plastic products. The demand of propylene has been growing in the global chemical industry in recent years.<sup>1,2</sup> With the increasing demand of propylene, several propylene production technologies including catalytic and thermal crackers,<sup>3</sup> methanol to olefins,<sup>4</sup> propane dehydrogenation<sup>5</sup> and olefin metathesis,<sup>6</sup> are available. Nowadays, olefin metathesis has become more interesting because it could regulate the stock of light olefins (ethylene, propylene, and butene) upon the market demand at low energy and environmental cost.<sup>7,8</sup> The olefin conversion technology (OCT) process licensed by Lummus Technology is the only commercial olefin metathesis technology producing propylene for the petrochemical industry, which used WO<sub>3</sub>/SiO<sub>2</sub> as a commercial catalyst to convert ethylene and 2-butene to propylene in a fixed-bed reactor at a temperature > 260 °C and pressure of 30–35 bar.<sup>2</sup> The WO<sub>3</sub>/SiO<sub>2</sub> catalysts are the most widely used catalysts because of their better resistance to poisoning, lower price, better stability and easy regeneration.<sup>8,9</sup>

The catalytic performance of WO<sub>3</sub>/SiO<sub>2</sub> catalysts for propylene metathesis is dependent on many parameters including the tungsten loading content, tungsten oxide species,

preparation conditions, support properties, and pretreatment conditions.<sup>8,10–15</sup> Among them, it was reported that the tungsten dispersion, tetrahedral tungsten oxide species, intermediate WO<sub>3-x</sub>, or W<sup>5+</sup> species are the active sites for metathesis,<sup>16–19</sup> and that WO<sub>3</sub> crystals are not active in metathesis and catalyst sites should be contained in the amorphous surface.<sup>8,20</sup> At present, the activation by pretreatment conditions to improve performance of supported WO<sub>x</sub>/SiO<sub>2</sub> catalysts in metathesis reaction has received much attention because of pre-activating the active sites of catalysts to form the activated state before running the reaction.<sup>21,22</sup> Pretreatment of supported WO<sub>3</sub>/SiO<sub>2</sub> catalysts with CO<sub>2</sub>, H<sub>2</sub> or N<sub>2</sub> gas at around 600 °C could improve the propylene self-metathesis activity.<sup>23–25</sup> Liu *et al.*<sup>13</sup> reported that H<sub>2</sub> content for pretreatment at 400 °C on the calcined WO<sub>3</sub>/SiO<sub>2</sub> catalysts caused the catalyst transformed to the tetragonal WO<sub>3</sub> and partially reduced W<sub>2.92</sub>, which were active phases for the metathesis of 1-butene and ethylene. In our previous research,<sup>8</sup> we have studied on the effect of pretreatment atmosphere over the calcined and non-calcined WO<sub>3</sub>/SiO<sub>2</sub> catalysts for the metathesis of ethylene and 2-butene to propylene by varying the gas pretreatment including pure N<sub>2</sub>, pure H<sub>2</sub> and mixed H<sub>2</sub>/N<sub>2</sub>, and using the pretreatment temperature of 500 °C. It was found that pure H<sub>2</sub> pretreatment over the non-calcined WO<sub>3</sub>/SiO<sub>2</sub> catalysts exhibited the WO<sub>2.83</sub> phase, which offered higher catalytic performance in the metathesis of ethylene and 2-butene. However, this research found the slightly inclined activity through time on stream of 12 h. To improve the catalytic performance, the research for hydrogen

Center of Excellence on Catalysis and Catalytic Reaction Engineering, Department of Chemical Engineering, Faculty of Engineering, Chulalongkorn University, Bangkok 10330, Thailand. E-mail: suttichai.a@chula.ac.th; Fax: +66-2218-6877; Tel: +66-2218-6868



pretreatment at elevated temperature have thus been investigated in the present research.

In this research, the effects of calcination and pretreatment temperatures on catalytic activities and stability of the H<sub>2</sub>-treated WO<sub>3</sub>/SiO<sub>2</sub> catalysts were studied for metathesis of ethylene and 2-butene to propylene. The catalyst activity was performed at the pressure of 20 bar, temperature of 350 °C and WHSV of 0.52 h<sup>-1</sup>. The properties of the catalysts were characterized by the Brunauer–Emmett–Teller (BET) method of N<sub>2</sub> physisorption, X-ray diffraction (XRD), transmission electron microscopy (TEM), diffuse reflectance ultraviolet-visible spectra (UV-Vis DRS), Raman microscopy, diffuse reflectance infrared Fourier transform spectroscopy of ammonia with *in situ* pretreatment (*in situ* NH<sub>3</sub>-DRIFTS), temperature-programmed desorption of ammonia with *in situ* pretreatment (*in situ* NH<sub>3</sub>-TPD) and temperature-programmed reduction of hydrogen with *in situ* pretreatment (*in situ* H<sub>2</sub>-TPR) to investigate the relationship of activity and stability, textural properties and dispersion of the catalysts, the structure of surface tungsten compounds, the acidity of the catalyst, and the interaction of tungsten species on support.

## 2. Experimental

### 2.1 Catalyst preparation

Silica gel, Davisil Grade 646 (40–60 mesh, supplied by “Aldrich”) was used as support. The precursor of 9 wt% WO<sub>3</sub>/SiO<sub>2</sub> catalysts was prepared by wetness impregnation using an aqueous solution of ammonium metatungstate hydrate (“Aldrich”, 99.9%). The impregnated sample was dried at room temperature for 2 h and subsequently in an oven at 110 °C for 24 h. Two types of the catalysts as the calcined and non-calcined catalysts were used for

further pretreatment and reaction testing. The calcined catalysts considered by using two calcination temperatures (550 and 650 °C) were performed at a desired temperature (550 or 650 °C) in air for 8 h, and then the catalysts were packed in a fixed bed reactor for further pretreatment and reaction. For the non-calcined catalysts, the samples after drying were packed in a fixed bed reactor for further hydrogen pretreatment and reaction.

### 2.2 Hydrogen pretreatment and catalytic performance evaluation

The metathesis of ethylene and 2-butene to propylene was performed in a tubular fixed-bed reactor (stainless steel, internal diameter = 19.05 mm). The 9% wt WO<sub>3</sub>/SiO<sub>2</sub> catalyst with the calcined or non-calcined catalyst of 3 g was packed at the center of the tubular fixed-bed reactor. The sample was heated to a pretreatment temperature (400, 500, 550, 600, 650 or 700 °C) by a furnace under N<sub>2</sub> gas at a flow rate of 30 ml min<sup>-1</sup> and held at the pretreatment temperature for 1 h. After that, pure H<sub>2</sub> gas at a total flow rate of 30 ml min<sup>-1</sup> was fed to the reactor for 1 h. The reactor was then cooled down to operating temperature of 350 °C under N<sub>2</sub> gas at the same flow rate. The reaction was started by introducing a feed containing 4% 2-butene (2% *cis*-2-butene and 2% *trans*-2-butene) and 8% ethylene balanced in nitrogen gas. The reaction condition was kept at the temperature of 350 °C, pressure of 20 bar and WHSV of 0.52 h<sup>-1</sup>. The catalysts were denoted as W-calxxx-Tyyy and W-nonal-Txxx representing the H<sub>2</sub>-treated calcined and non-calcined catalyst where “xxx” represents the calcination temperature including 550 and 650 for the temperature of 550 and 650 °C, while “yyy” represents the pretreatment

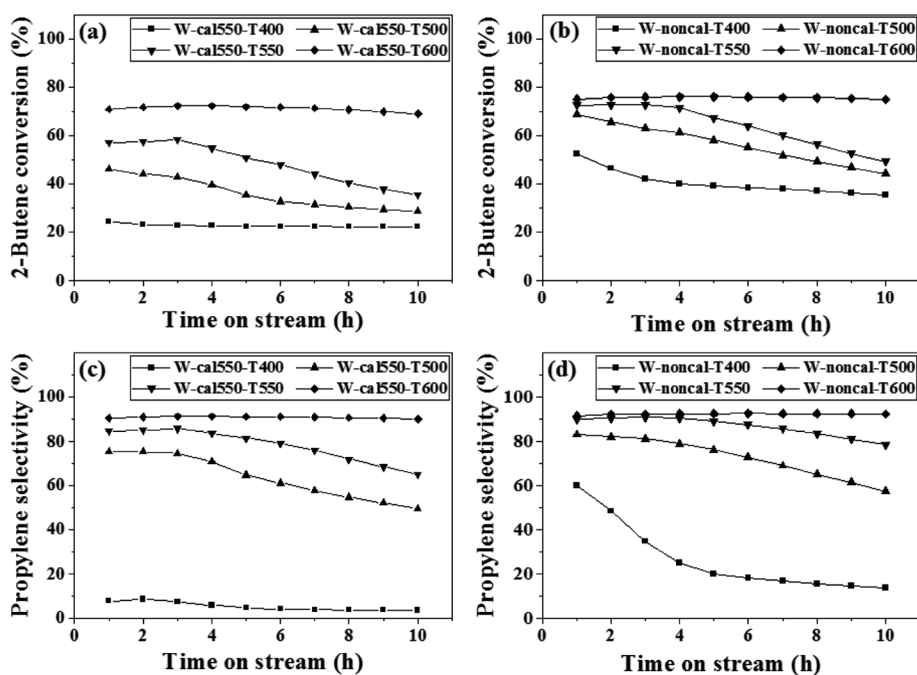


Fig. 1 Effect of pretreatment temperature on reaction performance of the calcined and non-calcined WO<sub>3</sub>/SiO<sub>2</sub> catalysts: (a) 2-butene conversion of the calcined catalysts at 550 °C, (b) 2-butene conversion of the non-calcined catalysts, (c) propylene selectivity of the calcined catalysts at 550 °C, and (d) propylene selectivity of the non-calcined catalysts ( $T = 350$  °C,  $P = 20$  bar, WHSV = 0.52 h<sup>-1</sup>).



temperature including 400, 500, 550, 600, 650 and 700 for the temperature of 400, 500, 550, 600, 650 and 700 °C, respectively.

All of the products were analyzed online by a gas chromatography (Agilent 7820A) with a HP-plot/Al<sub>2</sub>O<sub>3</sub> KCl column, which was equipped with a flame ionization detector (FID). The reaction pathways involved for metathesis reaction of ethylene and 2-butene to propylene were illustrated in our previous research.<sup>8</sup> The 2-butene conversion and product selectivity were determined by the following equations:

$$C_{2\text{-butene}} = \frac{[C_{2\text{-butene}}]_{\text{in}} - [C_{2\text{-butene}}]_{\text{out}}}{[C_{2\text{-butene}}]_{\text{in}}}$$

$$S_n = \frac{[C_n]}{\sum_{n=1}^5 [C_n]}$$

where  $C_{2\text{-butene}}$  and  $S_n$  are the 2-butene conversion and product selectivity of  $n$  (1 = propylene, 2 = 1-butene, 3 = isobutene, 4 = pentene and 5 = hexene), and where  $[C_{2\text{-butene}}]_{\text{in}}$ ,  $[C_{2\text{-butene}}]_{\text{out}}$  and  $[C_n]$  are the molar percentage of 2-butene at inlet, 2-butene at outlet and product of  $n$  (1 = propylene, 2 = 1-butene, 3 = isobutene, 4 = pentene and 5 = hexene), respectively.

### 2.3 Catalyst characterization

Brunauer-Emmett-Teller (BET) surface areas, pore volumes and pore sizes of all catalysts were measured by using Micro-metrics Chemisorbs 2750 with nitrogen adsorption studies. The X-ray diffraction (XRD) patterns of the catalysts were recorded on a D8 Advance of Bruker AXS using Ni-filter Cu K $\alpha$  radiation in the  $2\theta$  range of 20° to 80°. For phase composition identification purposes, the diffraction patterns were matched with standard diffraction data in JCPDS files. The Raman spectra of the

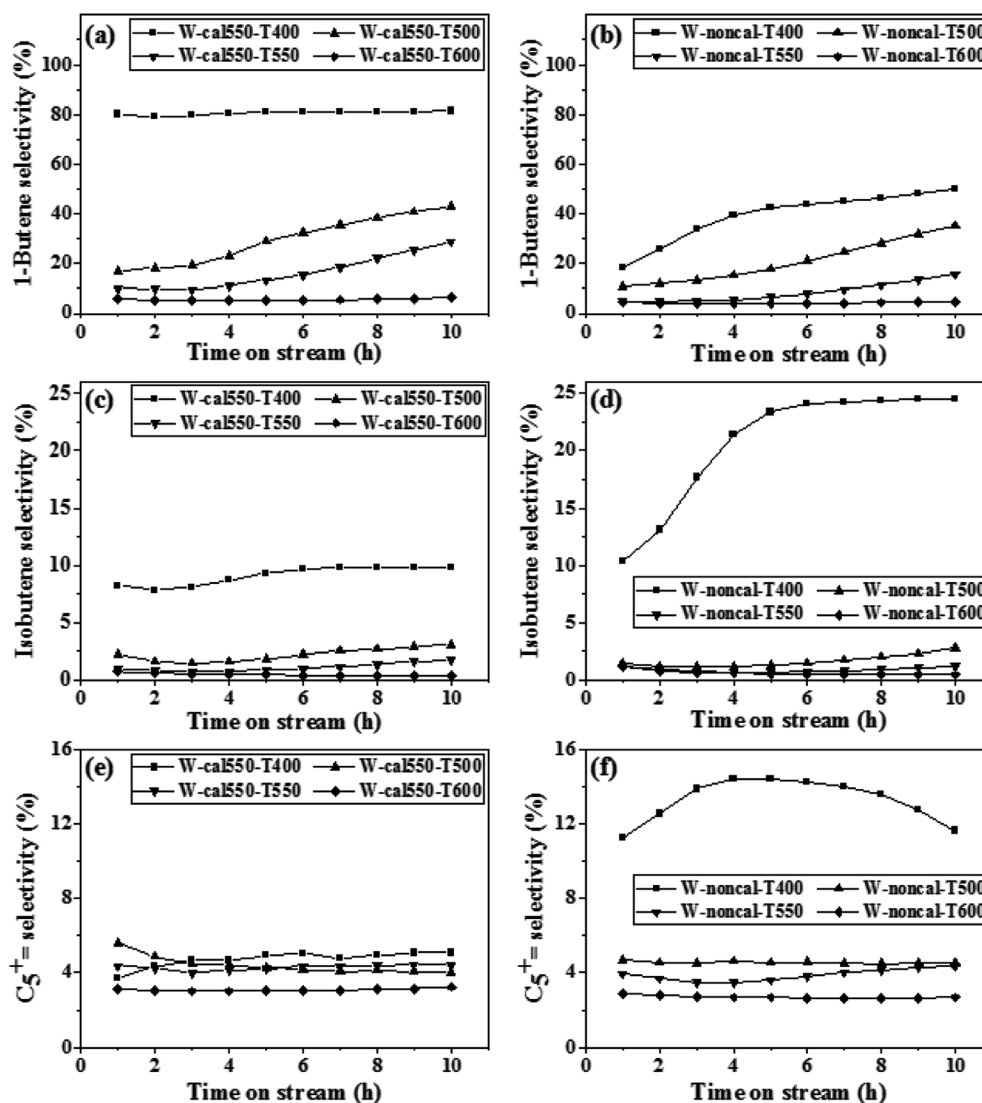


Fig. 2 Effect of pretreatment temperature on side product selectivity of the calcined and non-calcined WO<sub>3</sub>/SiO<sub>2</sub> catalysts: (a) 1-butene selectivity of the calcined catalysts at 550 °C, (b) 1-butene selectivity of the non-calcined catalysts, (c) isobutene selectivity of the calcined catalyst at 550 °C, (d) isobutene selectivity of the non-calcined catalysts, (e) C<sub>5</sub><sup>+</sup> selectivity of the calcined catalysts at 550 °C, and (f) C<sub>5</sub><sup>+</sup> selectivity of the non-calcined catalysts ( $T = 350$  °C,  $P = 20$  bar,  $WHSV = 0.52$  h<sup>-1</sup>).



samples were recorded under ambient conditions using a Senterra Dispersive Raman Microscopy (Bruker Optics) equipped with the laser wavelength at 532 nm and a TE-cooled CCD detector. The diffuse reflectance ultraviolet-visible spectra (UV-Vis DRS) was recorded on Lambda 650 spectrophotometer in the range between 200 and 800 nm.

The transmission electron microscopy (TEM) images was conducted on a JEOL JEM-2010 microscope equipped with a LaB<sub>6</sub> electron gun in the voltage range of 200 kV. The samples were prepared by dispersing in ethanol by sonication and a few drops of suspension onto a carbon-coated copper grid followed by solvent evaporation in air at room temperature.

The *in situ* diffuse reflectance infrared Fourier transform spectroscopy (*in situ* DRIFTS) of ammonia (NH<sub>3</sub>) adsorption spectra at various pretreatment temperature (400, 500, 550, 600, 650 and 700 °C) with H<sub>2</sub> gas over the two type catalysts as the calcined and non-calcined catalysts were recorded with a Bruker Vertex-70 FT-IR spectrometer equipped with a Harrick Praying Mantis attachment for diffuse reflectance spectroscopy. Diffuse reflectance measurements were performed *in situ* in a high temperature cell equipped with a KBr windows. The sample about 40–50 mg was placed in the Harrick cell, which were cooled by flowing water. The catalyst was heated to a desired pretreatment temperature (400, 500, 550, 600, 650 and 700 °C) under a N<sub>2</sub> flow rate of 10 ml min<sup>-1</sup> with a heating rate of 10 °C min<sup>-1</sup>, and then the pure H<sub>2</sub> gas at a flow rate of 1 ml min<sup>-1</sup> was fed to the cell for 0.5 h. After that, the sample was cooled down to 40 °C under a N<sub>2</sub> flow rate of 10 ml min<sup>-1</sup>. Subsequently, it was exposed to a 15% NH<sub>3</sub>/He mixed gas with a flow rate of 10 ml min<sup>-1</sup> for 30 min, and the sample was then purged with a N<sub>2</sub> gas stream (10 ml min<sup>-1</sup>) for 1 h. The spectra were collected using a Mercury-Cadmium-Telluride (MCT) detector with a resolution of 4 cm<sup>-1</sup> and an accumulation of 128 scans.

Temperature-programmed reduction of hydrogen with *in situ* pretreatment (*in situ* H<sub>2</sub>-TPR) was performed by using a Micromeritic Chemisorb 2750 automated system with the *in situ* pretreatment measurement. The catalyst of 0.1 g was loaded into a quartz U-tube reactor. Prior to H<sub>2</sub>-TPR experiment, the sample was pretreated under a N<sub>2</sub> flow rate of 25 ml min<sup>-1</sup> with a heating rate of 10 °C min<sup>-1</sup> to a desired pretreatment temperature (400, 500, 550, 600, 650 and 700 °C), and then the pure H<sub>2</sub> gas at a flow rate of 1 ml min<sup>-1</sup> was fed to the reactor for 1 h. After that, the reactor was cooled down to 40 °C under a N<sub>2</sub> flow rate of 25 ml min<sup>-1</sup>. Subsequently, the catalyst was reduced by using 10% H<sub>2</sub>/Ar with a flow rate of 25 ml min<sup>-1</sup> at a heating rate of 10 °C min<sup>-1</sup> from 40 to 900 °C. The amount of hydrogen uptake was determined by measuring the areas of the reduction profiles on the thermal conductivity detector (TCD).

Temperature-programmed desorption of ammonia with *in situ* pretreatment (*in situ* NH<sub>3</sub>-TPD) was used to determine the acidity of catalysts by a Micromeritic Chemisorb 2750 automated system with the *in situ* pretreatment measurement. The catalyst of 0.1 g packed in a quartz U-tube reactor was pretreated under a N<sub>2</sub> flow rate of 25 ml min<sup>-1</sup> with a heating rate of 10 °C min<sup>-1</sup> to a desired pretreatment temperature (400, 500, 550, 600, 650 and 700 °C), and then the pure H<sub>2</sub> gas at a flow rate of 1 ml min<sup>-1</sup> was fed to the reactor for 1 h. After that, the

sample was cooled down to 40 °C under a N<sub>2</sub> flow rate of 25 ml min<sup>-1</sup>. Subsequently, it was exposed to a 15% NH<sub>3</sub>/He mixed gas with a flow rate of 25 ml min<sup>-1</sup> for 30 min, and the sample was then purged with a He gas stream (25 ml min<sup>-1</sup>) for 1 h and the temperature was increased linearly with a rate of 10 °C min<sup>-1</sup> to 500 °C. The desorbed ammonia was detected by using the thermal conductivity detector (TCD).

## 3. Results and discussion

### 3.1 Catalytic performance in the metathesis of ethylene and 2-butenes

The metathesis performance was illustrated by varying the pretreatment temperature (400, 500, 550, 600, 650 and 700 °C) with pure H<sub>2</sub> gas on the calcined and non-calcined catalysts in the metathesis of 2-butene (*trans*- and *cis*-) and ethylene to propylene. The reaction was operated at 350 °C, 20 bar and 0.52 h<sup>-1</sup> of WHSV with the reactant of 2% *cis*-2-butene, 2% *trans*-2-butene and 8% ethylene in balanced N<sub>2</sub>. The 2-butene conversion and propylene selectivity for the H<sub>2</sub>-treated calcined catalysts at a calcination temperature of 550 °C and non-calcined catalysts are shown in Fig. 1. The results showed that increasing hydrogen pretreatment temperature exhibited higher 2-butene conversion and propylene selectivity for both calcined and non-calcined catalysts. In addition, the catalytic performance at the pretreatment temperature of 600 °C were stable for 10 h operation for both calcined and non-calcined catalysts. In comparison between the calcined catalysts with calcination temperature of 550 °C and non-calcined catalysts, it was found that the H<sub>2</sub> pretreatment of the non-calcined catalyst exhibited the 2-butene conversion and propylene selectivity higher than the calcined catalysts at any pretreatment temperature. The initial 2-butene conversion and propylene selectivity showed the same trend as the following order: W-noncal-T600 > W-noncal-T550 > W-cal550-T600 > W-cal550-

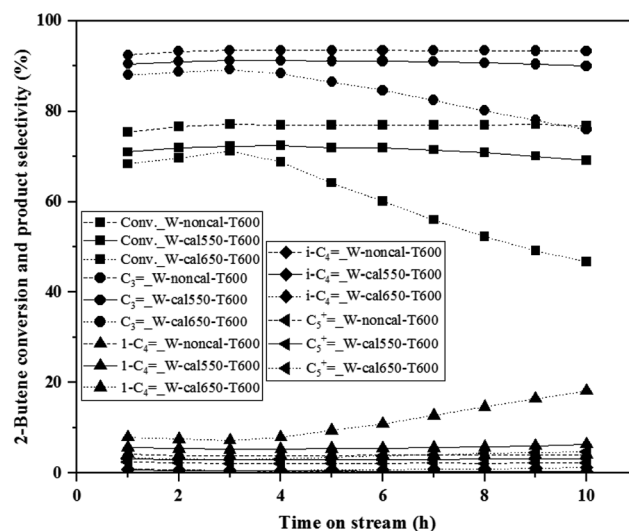


Fig. 3 Effect of calcination temperature on reaction performance of the WO<sub>3</sub>/SiO<sub>2</sub> catalysts with hydrogen pretreatment at 600 °C ( $T = 350$  °C,  $P = 20$  bar,  $WHSV = 0.52$  h<sup>-1</sup>).



T550 > W-cal550-T500 > W-noncal-T400 > W-cal550-T400. Considering the side product selectivity (Fig. 2), it was found that increasing H<sub>2</sub> pretreatment temperature lowered 1-butene, isobutene, and C<sub>5</sub><sup>+</sup> selectivities but those of the non-calcined catalysts was lower than the calcined catalysts, except the non-calcined catalyst with hydrogen pretreatment temperature of 400 °C, which exhibited the highest side products.

Interestingly, when considering the results of the hydrogen pretreatment at 600 °C, it was found that the catalytic performance and stability of the calcined catalyst (550 °C) were close to the non-calcined catalyst. It should be noted that generally, calcination of the catalysts was used to reduce the effect of impurities or remove volatile substances from preparation methods,<sup>26,27</sup> while catalyst pretreatment was used to obtain the active sites forming before the reaction running,<sup>22</sup> and the pretreatment temperature was usually lower than the calcination temperature. In further studies, the calcination

temperature of 650 °C, which was higher than pretreatment temperature of 600 °C, was also investigated. The catalytic performances of the calcined catalysts at calcination temperatures of 550 and 650 °C, and the non-calcined catalysts with hydrogen pretreatment temperature at 600 °C are shown in Fig. 3. It was found that the calcined catalyst with the calcination temperature of 550 °C exhibited the activity and stability higher than that of 650 °C, but still lower than the non-calcined catalyst with the same pretreatment temperature. These results confirmed that the pretreatment temperature of 600 °C on the non-calcined catalyst exhibited the activity and stability of metathesis reaction higher than the calcined catalyst, and the hydrogen pretreatment at a temperature higher than the calcination temperature also exhibited better activity and stability than the higher calcination temperature of the calcined catalyst at the same hydrogen pretreatment temperature, and almost close to the non-calcined catalyst. Therefore, the improvement of metathesis reaction of ethylene and 2-butene could be achieved by hydrogen pretreatment of the non-calcined catalysts or calcined catalyst with a calcination temperature lower than the pretreatment temperature. Fig. 4 shows the experimental results of the non-calcined catalysts at higher pretreatment temperatures (650 and 700 °C). It was found that the optimum hydrogen pretreatment temperature was at 650 °C, in which the highest 2-butene conversion and propylene selectivity, and the lowest side product selectivities including 1-butene, isobutene and C<sub>5</sub><sup>+</sup> were obtained. Such results suggested that the elevated temperature for hydrogen pretreatment over the calcined and non-calcined catalysts obviously affected the activity and stability of the catalysts, and the non-calcined catalyst pretreated with hydrogen at the temperature of 650 °C exhibited the highest activity and stability on the metathesis of ethylene and 2-butene to propylene.

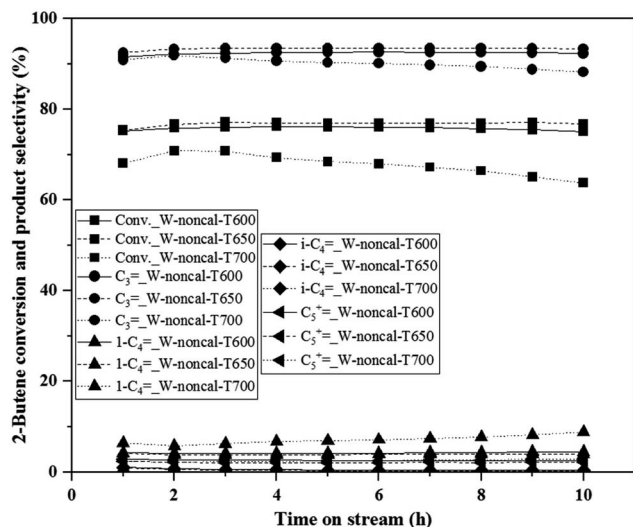


Fig. 4 Catalytic performance of hydrogen pretreatment under different temperatures of 600, 650 and 700 °C of the non-calcined WO<sub>3</sub>/SiO<sub>2</sub> catalysts ( $T = 350$  °C,  $P = 20$  bar; WHSV = 0.52 h<sup>-1</sup>).

### 3.2 Textural properties and dispersion of the catalysts

The N<sub>2</sub> adsorption–desorption isotherms and pore size distribution of the H<sub>2</sub> pretreatment on the calcined and non-calcined catalysts at different pretreatment temperatures are shown in

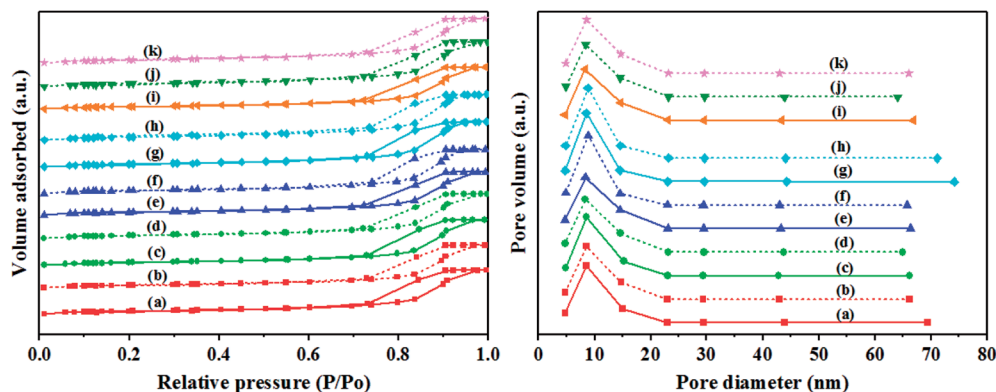


Fig. 5 N<sub>2</sub> adsorption–desorption isotherms (left) and pore size distributions (right) of the calcined (continuous lines) and non-calcined (short dashed lines) WO<sub>3</sub>/SiO<sub>2</sub> catalysts pretreated with pure H<sub>2</sub> at different temperatures: (a) W-cal550-T400, (b) W-noncal-T400, (c) W-cal550-T500, (d) W-noncal-T500, (e) W-cal550-T550, (f) W-noncal-T550, (g) W-cal550-T600, (h) W-noncal-T600, (i) W-cal650-T600, (j) W-noncal-T650 and (k) W-noncal-T700.



Fig. 5, and their textural properties are listed in Table 1. The isotherms of all catalysts showed typical IV isotherms with the H1 hysteresis loop, which revealed that all catalysts possessed a mesoporous structure.<sup>28,29</sup> The sharp capillary condensation feature at relative pressure of 0.75–0.95 ( $P/P_0$ ) indicated the existence of uniform pores in all catalysts. It could be clearly observed that all catalysts showed similar narrow pore size distributions (Fig. 5(right)). The specific surface area, pore volume, and average pore size of all catalysts (in Table 1) showed no significant differences within experimental error accepted around 5–10%. In other words, the pretreatment temperature did not affect much the physical properties of the calcined and non-calcined catalysts.

The XRD patterns of all pretreated catalysts are shown in Fig. 6. The catalysts obtained at various hydrogen pretreatment

temperatures showed the XRD patterns differently based on the standard reference data in JCPDS. For pretreatment temperature at 400 °C, the XRD patterns were assigned to tetragonal  $\text{WO}_3$  for the calcined catalysts and amorphous  $\text{WO}_3$  for the non-calcined catalysts, while those pretreated at 500 and 550 °C showed the  $\text{WO}_{2.92}$  phase for the calcined catalyst and  $\text{WO}_{2.83}$  phase for the non-calcined catalyst, and those pretreated at equal or higher than 600 °C showed the multiple phase compositions for both calcined and non-calcined catalysts. The hydrogen pretreatment at 600 °C for the calcined catalysts with the calcination temperature of 550 and 650 °C showed the  $\text{WO}_{2.92}$ ,  $\text{WO}_{2.83}$  and  $\text{WO}_2$  phase composition, whereas the patterns of the calcination at 550 °C exhibited lower crystallinity, indicating the better dispersed tungsten species on the surface.<sup>8</sup> For the hydrogen pretreatment at equal and higher than 600 °C on the non-calcined catalysts, the XRD patterns for the pretreatment temperature of 600 °C showed the  $\text{WO}_{2.83}$  and  $\text{WO}_2$  phase composition and that of 650 °C showed the  $\text{WO}_{2.83}$ ,  $\text{WO}_2$  and  $\text{W}^0$  phase composition, while that of 700 °C showed the  $\text{WO}_2$  and  $\text{W}^0$  phase composition. In addition, it was found that the XRD patterns of the non-calcined catalyst at pretreatment of 650 °C exhibited lower crystallinity than those of other pretreatment temperatures, indicating the higher dispersion of W species on the support.<sup>26</sup>

The particle morphology and lattice spacing of the samples were investigated by TEM and HRTEM images and the results are shown in Fig. 7. For the TEM images, it was found that increasing hydrogen pretreatment temperature exhibited the better tungsten dispersion on the surface catalysts, as indicated by fewer agglomerates than the lower pretreatment temperature. For any pretreatment temperature, the  $\text{H}_2$ -treated non-calcined catalysts showed fewer agglomerates than the  $\text{H}_2$ -

Table 1 BET surface areas, pore volumes and pore sizes of different  $\text{WO}_3/\text{SiO}_2$  catalysts

Catalysts	BET surface area ( $\text{m}^2 \text{g}^{-1}$ )	Pore volume ( $\text{cm}^3 \text{g}^{-1}$ )	Pore size (nm)
W-cal550-T400	286	0.98	9.35
W-cal550-T500	287	1.04	9.21
W-cal550-T550	289	0.98	9.19
W-cal550-T600	294	1.05	8.85
W-cal650-T600	266	0.98	9.53
W-noncal-T400	288	0.97	9.49
W-noncal-T500	298	1.03	9.45
W-noncal-T550	300	1.01	8.98
W-noncal-T600	316	1.07	9.08
W-noncal-T650	303	1.02	9.15
W-noncal-T700	296	1.02	9.48

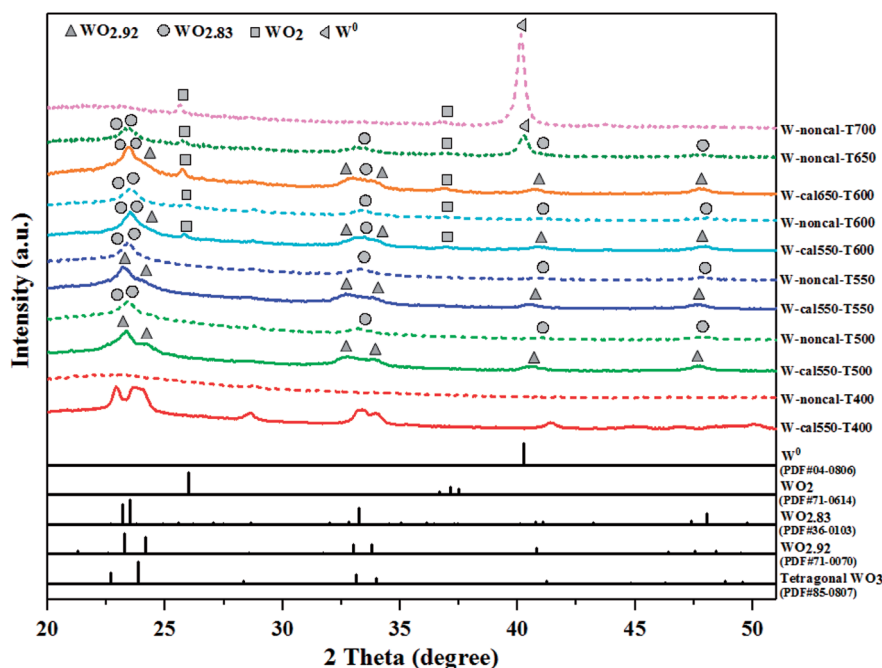


Fig. 6 XRD patterns of the calcined (colored continuous lines) and non-calcined (short dashed lines)  $\text{WO}_3/\text{SiO}_2$  catalysts with pure  $\text{H}_2$  pretreatment at different temperatures and standard reference data from JCPDS (black continuous lines).



treated calcined catalysts. As revealed by the high resolution TEM images (inset figure), it was found only one kind of the crystal lattice planes for the H<sub>2</sub>-treated calcined and non-calcined catalysts at temperature of 400, 500 and 550 °C, except the H<sub>2</sub>-treated non-calcined catalyst at temperature of 400 °C, in which the crystal lattice planes were not found due to its amorphous structure.<sup>8</sup> Whilst for the H<sub>2</sub>-treated calcined and non-calcined catalysts at temperature of 600 °C, various crystal lattice planes were found. Nevertheless, the pretreatment temperature at 650 and 700 °C of the non-calcined catalyst illustrated the three and two kinds of the crystal lattice planes also. The lattice spacing of all catalysts revealed the spacing at around 0.22, 0.34, 0.38 and 0.39 nm, which were consistent with the XRD standard reference data in JCPDS. The lattice spacing of the (001) planes of tetragonal WO<sub>3</sub>, (010) planes of WO<sub>2.92</sub>, (010) planes of WO<sub>2.83</sub>, (011) planes of WO<sub>2</sub> and (110) planes of W<sup>0</sup> were about 0.392, 0.382, 0.379 and 0.343 nm, respectively.

### 3.3 Structure of surface tungsten compounds

Structure of tungsten species produced by pure H<sub>2</sub> gas pretreatment at different pretreatment temperatures on the calcined and non-calcined catalysts were analyzed by UV-Vis DRS as shown in Fig. 8. Two absorption bands at 230 and 270 nm were observed in

the spectra for all the catalysts (inset figure), whereas the adsorption bands between 400 and 800 nm were also observed for all the catalysts. According to the literatures,<sup>8,15,17</sup> the absorption bands at 230 nm could be assigned to isolated tetrahedral [WO<sub>4</sub>]<sup>2-</sup> species, while the absorption bands at 270 nm corresponded to octahedral polytungstate species. The adsorption bands between 400 and 800 nm could be assigned to W<sup>4+</sup> and W<sup>5+</sup> species.<sup>17</sup> As shown in this figure, it was found that increasing the hydrogen pretreatment temperature affected the intensity of adsorption band at both 230 and 270 nm slightly increased, and these adsorption bands of the H<sub>2</sub>-treated non-calcined catalysts exhibited the intensities higher than the H<sub>2</sub>-treated calcined catalysts. The adsorption band between 400 and 800 nm of the catalysts was also broader with increasing the pretreatment temperature, and that of the H<sub>2</sub>-treated non-calcined catalysts at 700 °C showed the broadest ones, ascribed to the ordered mesoporous structure and enlarged oxygen vacancies due to higher W<sup>5+</sup> in sub-stoichiometric WO<sub>3-x</sub>,<sup>30</sup> which were consistent with the XRD results.

The Raman spectra of the H<sub>2</sub>-treated calcined and non-calcined catalysts at different pretreatment temperatures was also shown in Fig. 9. The bands at 263–275, 325–329, 701–720 and 801–810 cm<sup>-1</sup>, which were identified as the four strongest modes of tungsten oxide,<sup>30</sup> were assigned to the deformation mode of W–O–W, bending mode of O–W–O, bending mode of W–O, and symmetric

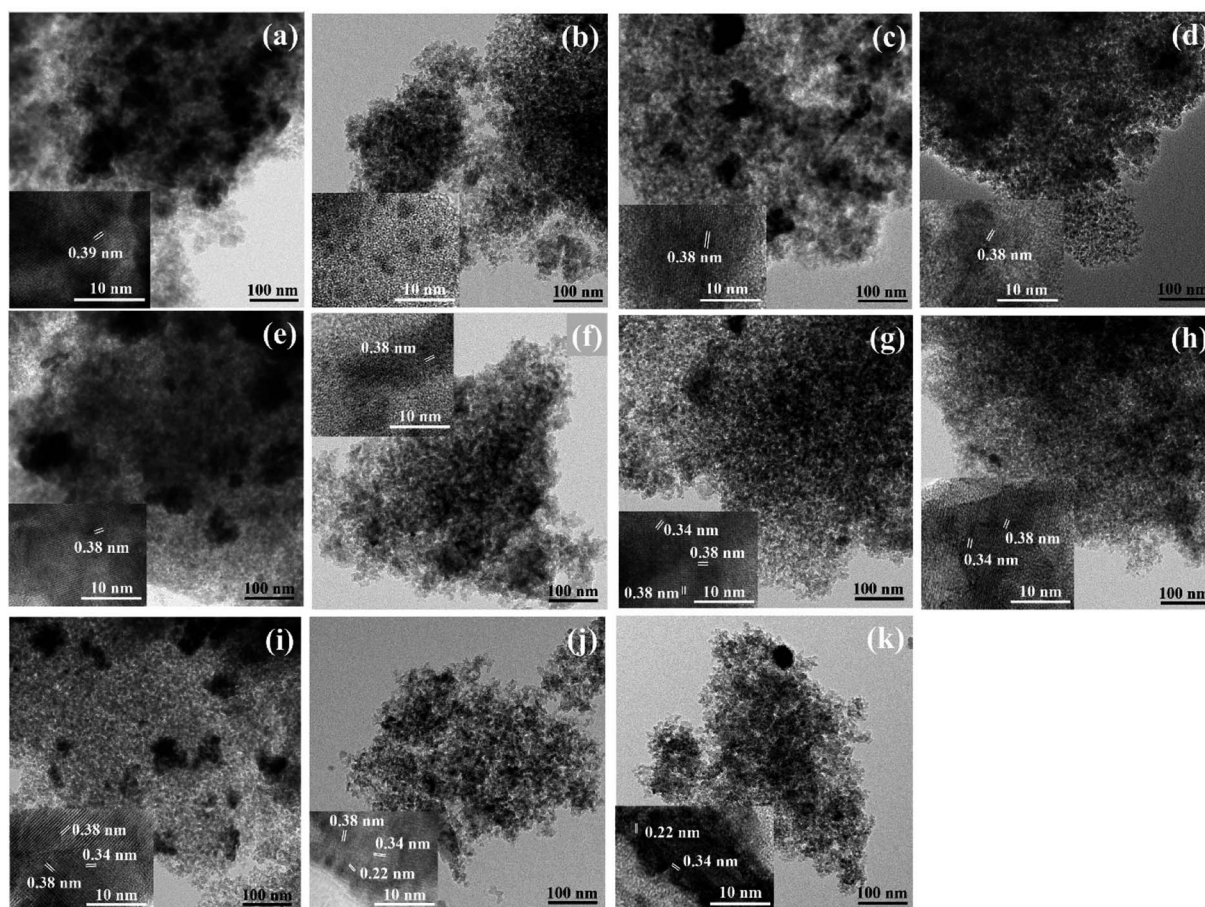


Fig. 7 TEM and HRTEM (inset) images of the calcined (top) and non-calcined (bottom) WO<sub>3</sub>/SiO<sub>2</sub> catalysts with pure H<sub>2</sub> pretreatment at different temperatures; (a) W-cal550-T400, (b) W-noncal-T400, (c) W-cal550-T500, (d) W-noncal-T500, (e) W-cal550-T550, (f) W-noncal-T550, (g) W-cal550-T600, (h) W-noncal-T600, (i) W-cal650-T600, (j) W-noncal-T650 and (k) W-noncal-T700.



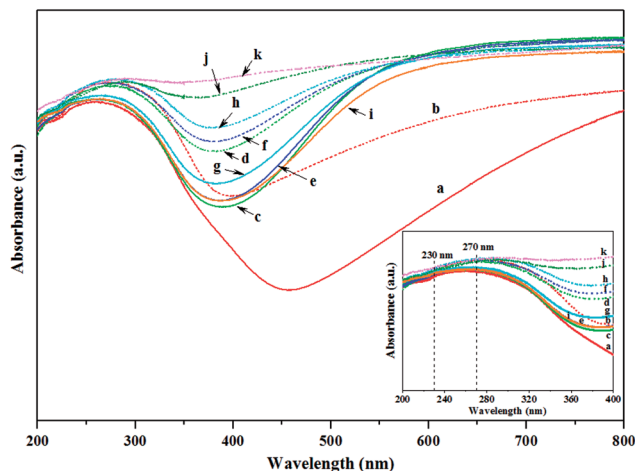


Fig. 8 UV-Vis DRS patterns of the calcined (continuous lines) and non-calcined (short dashed lines)  $\text{WO}_3/\text{SiO}_2$  catalysts pretreated with pure  $\text{H}_2$  at different temperatures; (a) W-cal550-T400, (b) W-nonal-T400, (c) W-cal550-T500, (d) W-nonal-T500, (e) W-cal550-T550, (f) W-nonal-T550, (g) W-cal550-T600, (h) W-nonal-T600, (i) W-cal650-T600, (j) W-nonal-T650 and (k) W-nonal-T700.

stretching mode of W–O, respectively.<sup>15,30,31</sup> The broad band at  $970\text{ cm}^{-1}$  was assigned to the O=W=O band of isolated surface tetrahedral tungsten oxide species.<sup>32</sup> The hydrogen pretreatment at different temperatures of all catalysts showed the four strongest peaks (263–275, 325–329, 701–720 and  $801\text{--}810\text{ cm}^{-1}$ ) of crystalline  $\text{WO}_3$  but the small broad peaks at  $970\text{ cm}^{-1}$  were different. The four strongest peaks of crystalline  $\text{WO}_3$  became broader with increasing the pretreatment temperature of the  $\text{H}_2$ -treated calcined and non-calcined catalysts, suggesting that there was a gradual degradation of the crystallinity upon increasing

pretreatment temperature due to an increasing amount of oxygen vacancies in the form of  $\text{WO}_{3-x}$  phase,<sup>30</sup> which were consistent with the XRD and UV-Vis results. In addition, these bands of the non-calcined catalysts were broader than the calcined catalysts, indicating that higher oxygen vacancies occurring on the  $\text{WO}_3$  crystalline.<sup>8</sup> Considering the Raman band at  $970\text{ cm}^{-1}$  of the calcined and non-calcined catalysts, it was found that this band of the non-calcined catalyst showed more obvious peaks than that of the calcined samples, indicating more isolated surface tetrahedral tungsten oxide species as also confirmed by the UV-Vis results. In addition, higher calcination temperature caused low intensity of the Raman band at  $970\text{ cm}^{-1}$ . The comparison of the ratios of relative Raman intensities of the peak at  $970$  to  $805\text{ cm}^{-1}$  ( $I_{970}/I_{805}$ ) are shown in table (inset in Fig. 9), which was an indicative of the relative amount of isolated surface tetrahedral tungsten oxide species (active sites) to  $\text{WO}_3$  crystal (non-active sites).<sup>8,33</sup> The high pretreatment temperature exhibited the higher  $I_{970}/I_{805}$  ratio in both calcined and non-calcined catalysts and the  $\text{H}_2$  pretreatment at  $650\text{ }^\circ\text{C}$  of the non-calcined catalyst exhibited the highest  $I_{970}/I_{805}$  ratio among the catalysts studied. Based on the characterization results described above, it was concluded that  $\text{H}_2$  pretreatment of the non-calcined catalysts exhibited higher amount of isolated surface tetrahedral tungsten oxide than the calcined ones and the  $\text{H}_2$  pretreatment at  $650\text{ }^\circ\text{C}$  of the non-calcined catalyst showed the highest amount of isolated surface tetrahedral tungsten oxide.

### 3.4 Acidity of the catalysts

To distinguish the differences in  $\text{NH}_3$  adsorption behaviors over the catalysts, induced by the hydrogen pretreatment temperature of the calcined and non-calcined  $\text{WO}_3/\text{SiO}_2$  catalysts, the *in situ* DRIFTS spectra of ammonia adsorption/desorption were performed under different pretreatment temperatures. Fig. 10 shows the  $\text{NH}_3$  adsorption in the region of  $1100\text{--}1800\text{ cm}^{-1}$  over the  $\text{H}_2$ -treated calcined and non-calcined catalysts at  $\text{NH}_3$  desorption temperature of  $40\text{ }^\circ\text{C}$ . Several kinds of  $\text{NH}_3$  species corresponding to different adsorption wavenumbers were observed after the catalysts exposed to ammonia gas. The bands at  $1463$  and  $1685\text{ cm}^{-1}$  could be assigned to Brønsted acid sites, while the bands at  $1230$ ,  $1280$ ,  $1315$  and  $1615\text{ cm}^{-1}$  could be assigned to Lewis acid sites,<sup>34–36</sup> and the acid amount of the total Brønsted (TB) and Lewis (TL) acid sites are shown in Fig. 11 and Table 2. It was found that increasing pretreatment temperature increased both Brønsted and Lewis acid sites for the calcined catalysts due to the formation of Si–O–W–OH species through the reaction of terminal silanols and surface  $\text{WO}_3$ .<sup>37</sup> However, at pretreatment temperature of  $400\text{ }^\circ\text{C}$ , the catalysts showed higher Lewis acid sites than the others. On the other hand, those of the non-calcined catalysts decreased with increasing of the hydrogen pretreatment temperature, which indicated that the formation of the Si–O–W–OH species for the non-calcined catalysts was probably due to the higher dispersion of  $\text{WO}_3$  on the support, which was consistent with the BET, XRD, and Raman results. Comparing the calcination temperature between  $550$  and  $650\text{ }^\circ\text{C}$  for the  $\text{H}_2$ -treated calcined catalysts, it was found that higher calcination temperature caused low Brønsted and Lewis acid sites. Considering the ratios of

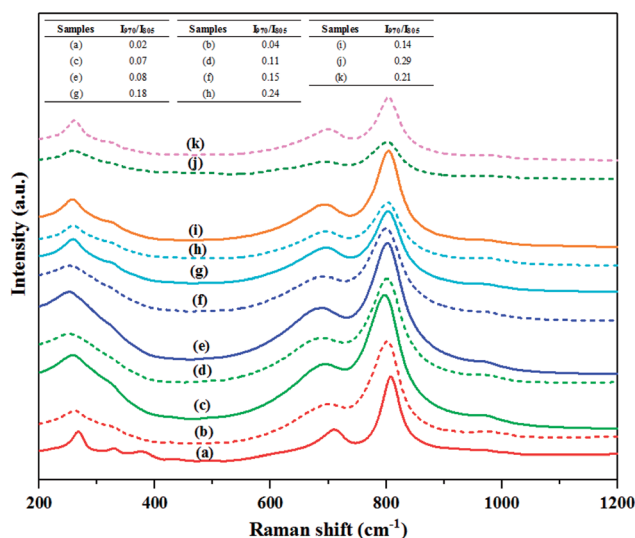


Fig. 9 Raman spectra of the calcined (continuous lines) and non-calcined (short dashed lines)  $\text{WO}_3/\text{SiO}_2$  catalysts pretreated with pure  $\text{H}_2$  at different temperatures; (a) W-cal550-T400, (b) W-nonal-T400, (c) W-cal550-T500, (d) W-nonal-T500, (e) W-cal550-T550, (f) W-nonal-T550, (g) W-cal550-T600, (h) W-nonal-T600, (i) W-cal650-T600, (j) W-nonal-T650 and (k) W-nonal-T700.





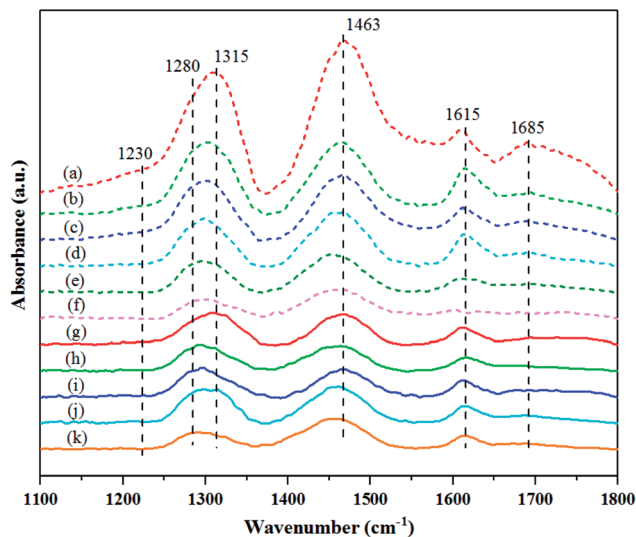


Fig. 10 *In situ*  $\text{NH}_3$ -DRIFTS profiles of the calcined (continuous lines) and non-calcined (short dashed lines)  $\text{WO}_3/\text{SiO}_2$  catalysts pretreated with pure  $\text{H}_2$  at different temperatures; (a) W-noncal-T400, (b) W-noncal-T500, (c) W-noncal-T550, (d) W-noncal-T600, (e) W-noncal-T650, (f) W-noncal-T700, (g) W-cal550-T400, (h) W-cal550-T500, (i) W-cal550-T550, (j) W-cal550-T600 and (k) W-cal650-T600.

Brønsted and Lewis acid sites (Table 2), it was found that the elevated pretreatment temperature of both  $\text{H}_2$ -treated calcined and non-calcined catalysts was likely to increase these ratios. And comparing the calcination temperature of 550 and 650 °C for the calcined catalysts pretreated at 600 °C, the calcination of 650 °C exhibited these ratios higher than that of 550 °C.

To investigate the total acidity of the catalyst, the  $\text{NH}_3$ -TPD was performed over the  $\text{H}_2$ -treated calcined and non-calcined catalysts with different pretreatment temperatures. The  $\text{NH}_3$ -TPD profiles are displayed in Fig. 12. The ammonia desorption peaks of the non-calcined  $\text{WO}_3/\text{SiO}_2$  catalysts occurred at higher temperature than the calcined catalysts, indicating the higher acid strength as stronger acidity.<sup>8,32</sup> In addition, increasing the pretreatment temperature caused the ammonia desorption peak to slightly shift to lower temperature, indicating lower acid strength.<sup>8</sup> Considering the amount of total acidity of all the catalysts as shown in Table 2, it was found that the amounts of total acidity of the  $\text{H}_2$ -treated calcined catalysts for calcination at 550 °C increased with increasing pretreatment temperature (except for pretreatment temperature at 400 °C that showed the total acidity amount higher than that at 500 and 550 °C, but less than that at 600 °C), while those of the non-calcined catalysts decreased with increasing the pretreatment temperature, which were consistent with the results of the *in situ* DRIFTS. In addition, comparing the calcination temperature of 550 and 650 °C for the calcined catalysts, it was found that higher calcination temperature caused low total amount of acidity, which was consistent with the *in situ* DRIFTS results.

### 3.5 Interaction of tungsten species on support

The  $\text{H}_2$ -TPR was performed to investigate the interaction between W active species and silica support and the profiles are

displayed in Fig. 13. The  $\text{H}_2$ -TPR profiles of the  $\text{H}_2$ -treated calcined and non-calcined  $\text{WO}_3/\text{SiO}_2$  catalysts showed three peaks at 495–505, 565, and 780–825 °C. The low temperature peaks were attributed to the reduction of W species in octahedral coordination and the high temperature peak was assigned to the reduction of the surface amorphous  $\text{WO}_3$  species.<sup>15,17</sup> Comparing between the calcined and non-calcined  $\text{WO}_3/\text{SiO}_2$  catalysts, the reduction peak at low temperature of the non-calcined catalysts appeared at higher temperature than the calcined ones, indicating that interaction of W species in octahedral coordination on silica support of the non-calcined catalysts was stronger than the calcined catalysts. Whilst the reduction peaks at high temperature of the non-calcined catalysts appeared at lower temperature than the calcined catalysts, indicating that reduction of  $\text{WO}_3$  crystal of the non-calcined catalysts was weaker than the calcined catalysts, which reflected an improved reducibility of dispersed species.<sup>15</sup> In addition, comparing the calcination temperature of 550 and 650 °C of the calcined catalysts, it was found that reduction peak at low temperature of the calcination of 650 °C appeared at higher temperature than that of 550 °C, while the reduction peak at high temperature was not significantly different. Interestingly, when the pretreatment temperature of the non-calcined catalysts higher than 600 °C, it was found that the reduction peak at low temperature shifted to higher temperature, and the pretreatment of 650 °C shifted the low temperature peak to higher temperature than that of 700 °C, indicating that higher interaction of tungsten species on the support.<sup>15</sup> In contrast, reduction peak at high temperature for the pretreatment temperature of 650 and 700 °C was slightly broad, and the pretreatment temperature of 700 °C was broader and shifted to lower temperature than that of 650 °C, which might be assigned to higher  $\text{W}^0$  formation<sup>15</sup> and was confirmed the  $\text{W}^0$  occurring by the XRD results. Considering the effect of hydrogen pretreatment temperature on the calcined and non-calcined catalysts, the increasing of the pretreatment temperature up to 600 °C led to a boarder low temperature peak, while the high temperature peaks of either calcined or non-calcined catalysts were not significantly different, and the low  $\text{H}_2$  consumption peaks (inset figure) shifted to lower temperature, except the pretreatment temperature of 600 °C on the calcined catalyst at 550 °C, which exhibited two peaks at low temperature and the lowest temperature peaks were shifted to higher temperature. In addition, pretreatment at 600 °C on the catalyst calcined at 650 °C could improve the interaction of tungsten species on the support, comparing with the same pretreatment temperature on the calcined catalyst at 550 °C. Furthermore, increasing pretreatment temperature higher than 600 °C for the  $\text{H}_2$ -treated non-calcined catalyst also led to higher interaction and  $\text{W}^0$  formation, which was consistent with the XRD, UV-Vis, and Raman results.

### 3.6 Structural–activity relationship

The effects of hydrogen pretreatment over the calcined and non-calcined  $\text{WO}_3/\text{SiO}_2$  catalysts were studied in the metathesis of ethylene and 2-butene at 20 bar and 350 °C. Different



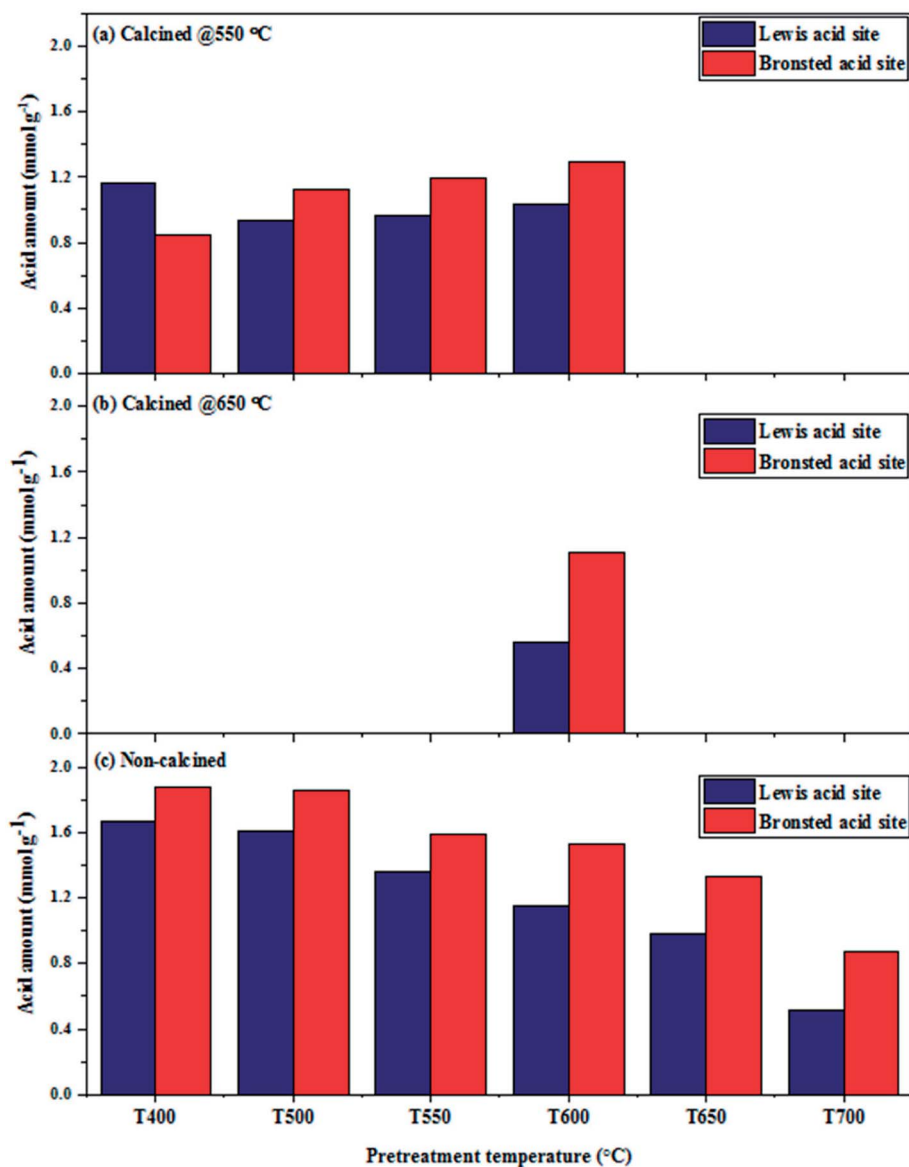


Fig. 11 The acid amount of Brønsted and Lewis acid sites of the calcined and non-calcined  $\text{WO}_3/\text{SiO}_2$  catalysts pretreated with pure  $\text{H}_2$  at different temperatures.

Table 2 The amount of total acidity, Brønsted and Lewis acid sites of different  $\text{WO}_3/\text{SiO}_2$  catalysts<sup>a</sup>

Samples	Total acidity <sup>b</sup> (mmol g <sup>-1</sup> )	Total Brønsted acid <sup>c</sup> (mmol g <sup>-1</sup> )	Total Lewis acid <sup>c</sup> (mmol g <sup>-1</sup> )	TB/TL
W-cal550-T400	2.20	0.84	1.16	0.72
W-cal550-T500	2.06	1.12	0.94	1.20
W-cal550-T550	2.13	1.19	0.96	1.23
W-cal550-T600	2.35	1.29	1.03	1.26
W-cal650-T600	1.68	1.11	0.56	2.00
W-noncal-T400	4.49	1.88	1.67	1.12
W-noncal-T500	3.73	1.86	1.61	1.16
W-noncal-T550	3.25	1.59	1.36	1.17
W-noncal-T600	2.72	1.53	1.15	1.33
W-noncal-T650	2.32	1.33	0.98	1.36
W-noncal-T700	1.54	0.87	0.51	1.71

<sup>a</sup> TB = total Brønsted acid sites and TL = total Lewis acid sites. <sup>b</sup> From *in situ*  $\text{NH}_3$ -TPD data calculation. <sup>c</sup> From *in situ*  $\text{NH}_3$ -DRIFTS data calculation.



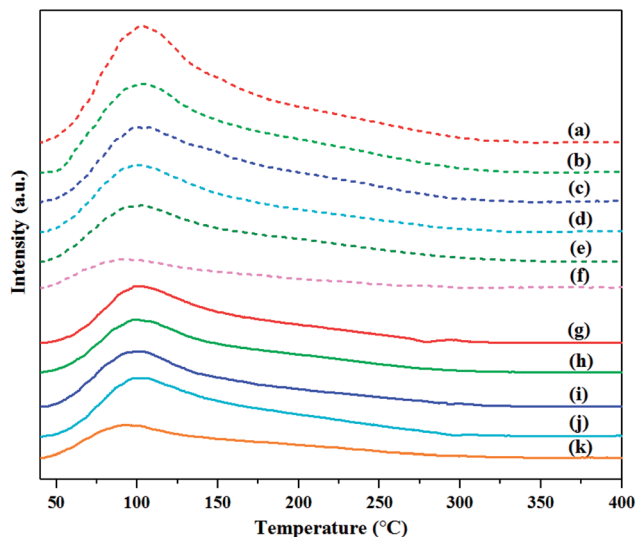


Fig. 12  $\text{NH}_3$ -TPD profiles of the calcined (continuous lines) and non-calcined (short dashed lines)  $\text{WO}_3/\text{SiO}_2$  catalysts with pure  $\text{H}_2$  pretreatment at different temperatures; (a) W-noncal-T400, (b) W-noncal-T500, (c) W-noncal-T550, (d) W-noncal-T600, (e) W-noncal-T650, (f) W-noncal-T700, (g) W-cal550-T400, (h) W-cal550-T500, (i) W-cal550-T550, (j) W-cal550-T600 and (k) W-cal650-T600.

pretreatment temperatures could lead to the changes of the textural properties and dispersion of the  $\text{WO}_3/\text{SiO}_2$  catalysts, the structure of surface tungsten compounds, the acidity of the catalyst, and the interaction of tungsten species on support. As revealed on the BET results, the specific surface area, pore volume and average pore size of all the catalysts occurring from

hydrogen pretreatment at elevated temperature was not much significant to affect the activity for the metathesis of ethylene and 2-butene. Considering the dispersion of tungsten on the silica support (as confirmed by XRD and TEM results), it was found that the  $\text{H}_2$ -treated non-calcined catalysts exhibited the activity higher than the  $\text{H}_2$ -treated calcined catalysts, and the pretreatment temperature at 650 °C of the  $\text{H}_2$ -treated non-calcined catalyst showed the highest activity, indicating that better dispersion of tungsten on the silica support exhibited the high activity of metathesis of ethylene and 2-butene to produce propylene.<sup>14,26,38</sup> Moreover, the TEM mapping results also confirmed that the  $\text{H}_2$ -treated calcined catalysts showed the more tungsten agglomerates dispersed on the surface silica support than the  $\text{H}_2$ -treated non-calcined catalysts, indicating poor tungsten dispersion on the support. Additionally, the UV-Vis and Raman results indicated that the higher amount of isolated tetrahedral tungsten oxide was active species for metathesis reaction.<sup>8,17</sup>

Considering the crystalline phase composition and average crystal size of the catalysts calculated by the Scherrer equation for the XRD results as shown in Table 3, it was found that increasing the pretreatment temperature of the  $\text{H}_2$ -treated calcined and non-calcined catalyst caused the different multiple phase compositions and decreased the average crystal size. When comparison with the initial 2-butene conversion, propylene and 1-butene selectivity (in Table 3) at operation of 1 h, it was found that the composition  $\text{WO}_{2.83}$  and  $\text{WO}_2$  phase on the pretreated catalysts caused the high 2-butene conversion and propylene selectivity, and lower the 1-butene selectivity. In addition, small crystal size of these phases also exhibited the high catalytic activity, which was related with higher tungsten

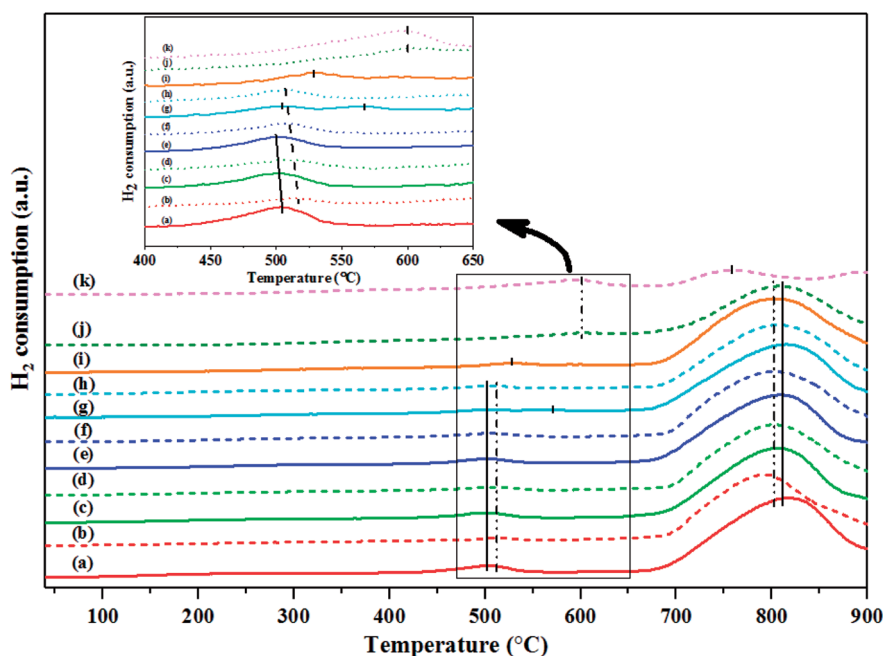


Fig. 13  $\text{H}_2$ -TPR patterns of the calcined (continuous lines) and non-calcined (short dashed lines)  $\text{WO}_3/\text{SiO}_2$  catalysts with *in situ* pure  $\text{H}_2$  pretreatment at different temperatures; (a) W-cal550-T400, (b) W-noncal-T400, (c) W-cal550-T500, (d) W-noncal-T500, (e) W-cal550-T550, (f) W-noncal-T550, (g) W-cal550-T600, (h) W-noncal-T600, (i) W-cal650-T600, (j) W-noncal-T650 and (k) W-noncal-T700.



**Table 3** The detailed parameters of XRD results and catalytic performance of 2-butene conversion, propylene and 1-butene selectivities at 1 h over the calcined and non-calcined  $\text{WO}_3/\text{SiO}_2$  catalysts pretreated with pure  $\text{H}_2$  at different temperatures

Catalysts	Phase	$2\theta$ ( $^\circ$ )	Crystal size (nm)	2-Butene conversion <sup>a</sup> (%)	Propylene selectivity <sup>a</sup> (%)	1-Butene selectivity <sup>a</sup> (%)	Isobutene selectivity <sup>a</sup> (%)
W-cal550-T400	Tetragonal $\text{WO}_3$	22.9	19.8	24.4	7.9	80.2	8.2
W-cal550-T500	$\text{WO}_{2.92}$	23.3	16.3	46.2	75.3	16.9	2.2
W-cal550-T550	$\text{WO}_{2.92}$	23.2	15.8	57.3	84.6	9.9	1.0
W-cal550-T600	$\text{WO}_{2.92}$	n.a.	n.a.	71.0	90.5	5.6	0.8
	$\text{WO}_{2.83}$	23.5	15.2				
	$\text{WO}_2$	25.8	33.3				
W-cal650-T600	$\text{WO}_{2.92}$	n.a.	n.a.	68.4	88.0	7.9	0.8
	$\text{WO}_{2.83}$	23.4	15.9				
	$\text{WO}_2$	25.7	35.1				
W-noncal-T400	Amorphous $\text{WO}_3$	n.a.	n.a.	52.6	59.8	18.6	10.4
W-noncal-T500	$\text{WO}_{2.83}$	23.4	14.5	68.8	86.2	7.3	1.5
W-noncal-T550	$\text{WO}_{2.83}$	23.4	14.2	72.7	89.9	4.9	1.2
W-noncal-T600	$\text{WO}_{2.83}$	23.5	13.0	75.3	91.6	4.4	1.1
	$\text{WO}_2$	25.9	32.4				
	$\text{WO}_{2.83}$	23.4	10.8	75.4	92.4	4.2	0.9
W-noncal-T650	$\text{WO}_2$	25.8	31.8				
	$\text{W}^0$	40.3	21.2				
	$\text{WO}_2$	25.6	34.3	68.1	90.8	6.5	0.2
W-noncal-T700	$\text{W}^0$	40.1	25.1				

<sup>a</sup> Data in operation of 1 h.

dispersion on the support.<sup>14,26</sup> Therefore, the two mentioned crystalline phases are good proxy (indicators) of the reducibility of the W oxide phase, which itself is related to dispersion.

Considering the acidity of catalysts (*in situ*  $\text{NH}_3$ -DRIFTS and  $\text{NH}_3$ -TPD results), it was found that the suitable amount of total acidity and acid sites (Brønsted and Lewis acid sites) exhibited the high stability on the metathesis reaction of ethylene and 2-butene to propylene, in which pretreatment of the non-calcined catalyst at 600 and 650  $^\circ\text{C}$ , and the calcined catalyst at 550  $^\circ\text{C}$  with pretreatment of 600  $^\circ\text{C}$  showed the best stability through 10 h operation. These results were supported by the literatures that reported that the increased Brønsted acid sites could help to promote the metathesis reaction of ethylene and 2-butene to propylene,<sup>12,17,37,39</sup> but high number of the Brønsted acid sites led to isomerization of 1-butene to isobutene.<sup>37</sup> On the other hand, increased Lewis acid sites could help to promote the isomerization of 1-butene to 2-butene,<sup>37,39</sup> and suitable amount of acid sites was important for the stable activity of olefin metathesis.<sup>39</sup> In addition, crystalline  $\text{WO}_3$  could catalyze some isomerization reactions, and easily resulted in the deactivation of catalysts.<sup>39,40</sup> In the catalytic performance for 1 h operation as shown in Table 3, it was found that the  $\text{H}_2$ -treated calcined catalyst at pretreatment temperature under 550  $^\circ\text{C}$  exhibited high isomerization, indicating that high crystalline  $\text{WO}_3$  caused high isomerization reaction of 2-butene to 1-butene and that of 1-butene to isobutene, while the  $\text{H}_2$ -treated non-calcined catalysts at pretreatment temperature under 550  $^\circ\text{C}$  also exhibited high isomerization, indicating that high Lewis and Brønsted acid sites caused high isomerization reaction of 2-butene to 1-butene and that of 1-butene to isobutene, respectively. Therefore, the suitable amount of total acidity and acid sites

(Brønsted and Lewis acid sites) played an important role to the stability in the metathesis of ethylene and 2-butene.

Considering the interaction of tungsten species on the support (*in situ*  $\text{H}_2$ -TPR results), it was found that the  $\text{H}_2$ -treated non-calcined catalysts exhibited stronger interaction than the  $\text{H}_2$ -treated calcined catalysts at any pretreatment temperature, and increasing the pretreatment temperature to 600  $^\circ\text{C}$  caused the interaction between tungsten species and silica support decreased for both calcined catalyst at calcination of 550  $^\circ\text{C}$  and non-calcined catalyst. However, pretreatment temperature higher than 600  $^\circ\text{C}$  caused the higher interaction between tungsten species and support. In addition, comparing the catalytic performances, it was found that the interaction between tungsten species and silica support occurred from the hydrogen pretreatment at elevated temperature on the catalysts did not have significant impact on activity and stability on metathesis reaction of ethylene and 2-butene to propylene. Nevertheless, considering the hydrogen pretreatment at the temperature of 600  $^\circ\text{C}$  on the calcined catalyst at calcination of 550  $^\circ\text{C}$ , it was found that the pretreatment temperature higher than the calcination temperature exhibited the catalytic performances and characterization close to the non-calcined catalyst at the same pretreatment temperature. Such results indicated that the pretreatment temperature on the calcined catalysts at higher than the calcination temperature (550  $^\circ\text{C}$ ) could improve the catalytic performances to be close to the non-calcined catalyst, which was more active in the metathesis of ethylene and 2-butene to produce propylene. In other words, the catalytic performances in metathesis of ethylene and 2-butene to produce propylene could be improved by using the hydrogen pretreatment at elevated temperature on the non-calcined catalyst.



## 4. Conclusions

The hydrogen pretreatment at elevated temperature of the calcined and non-calcined  $\text{WO}_3/\text{SiO}_2$  catalysts for metathesis reaction of ethylene and 2-butene to propylene was investigated. The catalytic activity and stability could be improved by the hydrogen pretreatment. The results showed that the non-calcined catalysts with hydrogen pretreatment temperature of 650 °C offered the highest activity and stability. The calcination of the catalyst was unnecessary and it showed adverse effects when the calcination temperature was higher than the hydrogen pretreatment temperature. The characterization results indicated that the better tungsten dispersion,  $\text{WO}_{2.83}$  and  $\text{WO}_2$  phase compositions, and higher isolated surface tetrahedral tungsten oxide species are favorable to the high activity of the metathesis reaction of ethylene and 2-butene to propylene, while the suitable amount of total acidity and acid sites of both Brønsted and Lewis acid sites played an important role to the stability of metathesis reaction. In addition, the textural properties and interaction between W species and silica support occurring from pretreatment temperature were not significant to the activity and stability.

## Conflicts of interest

There are no conflicts of interest to declare.

## Acknowledgements

The authors acknowledge the support from the Department of Chemical Engineering, Faculty of Engineering, Chulalongkorn University. Department of Chemical Engineering, Faculty of Engineering, Chulalongkorn University would like to acknowledge The Institutional Research Grant (The Thailand Research Fund), IRG 5780014, and Chulalongkorn University, Contract No. RES\_57\_411\_21\_076.

## References

- W. Jiang, R. Huang, P. Li, S. Feng, G. Zhou, C. Yu, H. Zhou, C. Xu and Q. Xu, *Appl. Catal., A*, 2016, **517**, 227–235.
- J. C. Mol, *J. Mol. Catal. A: Chem.*, 2004, **213**, 39–45.
- J. Towfighi, A. Niaei, R. Karimzadeh and G. Saedi, *Korean J. Chem. Eng.*, 2006, **23**, 8–16.
- M. Stöcker, *Microporous Mesoporous Mater.*, 1999, **29**, 3–48.
- F. Cavani, N. Ballarini and A. Cericola, *Catal. Today*, 2007, **127**, 113–131.
- X. Li, W. Zhang, S. Liu, L. Xu, X. Han and X. Bao, *J. Phys. Chem. C*, 2008, **112**, 5955–5960.
- D. P. Debecker, M. Stoyanova, U. Rodemerck and E. M. Gaigneaux, *J. Mol. Catal. A: Chem.*, 2011, **340**, 65–76.
- K. Gayapan, S. Sripinun, J. Panpranot, P. Praserthdam and S. Assabumrungrat, *RSC Adv.*, 2018, **8**, 11693–11704.
- A. Spamer, T. I. Dube, D. J. Moodley, C. van Schalkwyk and J. M. Botha, *Appl. Catal., A*, 2003, **255**, 153–167.
- A. G. Basrur, S. R. Patwardhan and S. N. Was, *J. Catal.*, 1991, **127**, 86–95.

- T. I. Bhuiyan, P. Arudra, M. M. Hossain, M. N. Akhtar, A. M. Aitani, R. H. Abudawoud and S. S. Al-Khattaf, *Can. J. Chem. Eng.*, 2014, **92**, 1271–1282.
- S. Chaemchuen, S. Phatanasri, F. Verpoort, N. Sae-ma and K. Suriye, *Kinet. Catal.*, 2012, **53**, 247–252.
- H. Liu, K. Tao, H. Yu, C. Zhou, Z. Ma, D. Mao and S. Zhou, *C. R. Chim.*, 2015, **18**, 644–653.
- N. Poovarawan, K. Suriye, J. Panpranot, W. Limsangkass, F. J. Santos Cadete Aires and P. Praserthdam, *Catal. Lett.*, 2015, **145**, 1868–1875.
- Q. Zhao, S.-L. Chen, J. Gao and C. Xu, *Transition Met. Chem.*, 2009, **34**, 621–627.
- S. J. Choung and S. W. Weller, *Ind. Eng. Chem. Process Des. Dev.*, 1983, **22**, 662–665.
- S. Huang, S. Liu, W. Xin, J. Bai, S. Xie, Q. Wang and L. Xu, *J. Mol. Catal. A: Chem.*, 2005, **226**, 61–68.
- H. Liu, S. Huang, L. Zhang, S. Liu, W. Xin and L. Xu, *Catal. Commun.*, 2009, **10**, 544–548.
- A. J. Van Roosmalen and J. C. Mol, *J. Catal.*, 1982, **78**, 17–23.
- S. Huang, F. Chen, S. Liu, Q. Zhu, X. Zhu, W. Xin, Z. Feng, C. Li, Q. Wang and L. Xu, *J. Mol. Catal. A: Chem.*, 2007, **267**, 224–233.
- K. Ding, A. Gulec, A. M. Johnson, T. L. Drake, W. Wu, Y. Lin, E. Weitz, L. D. Marks and P. C. Stair, *ACS Catal.*, 2016, **6**, 5740–5746.
- S. Lwin and I. E. Wachs, *ACS Catal.*, 2017, **7**, 573–580.
- A. Andreini and J. C. Mol, *J. Colloid Interface Sci.*, 1981, **84**, 57–65.
- R. C. Luckner, G. E. McConchie and G. B. Wills, *J. Catal.*, 1973, **28**, 63–68.
- R. Westhoff and J. A. Moulijn, *J. Catal.*, 1977, **46**, 414–416.
- S. Maksasithorn, P. Praserthdam, K. Suriye and D. P. Debecker, *Microporous Mesoporous Mater.*, 2015, **213**, 125–133.
- J. Thomas Richardson, *Principles of catalyst development*, 1991.
- C. Lin, K. Tao, H. Yu, D. Hua and S. Zhou, *Catal. Sci. Technol.*, 2014, **4**, 4010–4019.
- H. Liu, K. Tao, P. Zhang, W. Xu and S. Zhou, *New J. Chem.*, 2015, **39**, 7971–7978.
- L. Wang, Y. Wang, Y. Cheng, Z. Liu, Q. Guo, M. N. Ha and Z. Zhao, *J. Mater. Chem. A*, 2016, **4**, 5314–5322.
- Y. Wang, Q. Chen, W. Yang, Z. Xie, W. Xu and D. Huang, *Appl. Catal., A*, 2003, **250**, 25–37.
- S. Maksasithorn, D. P. Debecker, P. Praserthdam, J. Panpranot, K. Suriye and S. K. N. Ayudhya, *Chin. J. Catal.*, 2014, **35**, 232–241.
- W. Limsangkass, P. Praserthdam, S. Phatanasri, J. Panpranot, N. Poovarawan, W. Jareewatchara, S. Kunjara Na Ayudhya and K. Suriye, *Catal. Lett.*, 2014, **144**, 1524–1529.
- S. Vorakitkanvasin, W. Phongsawat, K. Suriye, P. Praserthdam and J. Panpranot, *RSC Adv.*, 2017, **7**, 38659–38665.
- H. Xu, M. Sun, S. Liu, Y. Li, J. Wang and Y. Chen, *RSC Adv.*, 2017, **7**, 24177–24187.
- X.-L. Yang, R. Gao, W.-L. Dai and K. Fan, *J. Phys. Chem. C*, 2008, **112**, 3819–3826.



- 37 G. Chen, M. Dong, J. Li, Z. Wu, G. Wang, Z. Qin, J. Wang and W. Fan, *Catal. Sci. Technol.*, 2016, **6**, 5515–5525.
- 38 S. Huang, S. Liu, Q. Zhu, X. Zhu, W. Xin, H. Liu, Z. Feng, C. Li, S. Xie, Q. Wang and L. Xu, *Appl. Catal., A*, 2007, **323**, 94–103.
- 39 N. Liu, S. Ding, Y. Cui, N. Xue, L. Peng, X. Guo and W. Ding, *Chem. Eng. Res. Des.*, 2013, **91**, 573–580.
- 40 D. P. Debecker, M. Stoyanova, U. Rodemerck, F. Colbeau-Justin, C. Boissère, A. Chaumonnot, A. Bonduelle and C. Sanchez, *Appl. Catal., A*, 2014, **470**, 458–466.

